Chemisorption on a FCC Metal Surface: Electronic Structure of Ordered Overlayers

Kin-ichi Masuda

Department of Materials Science and Engineering, Tokyo Institute of Technology, Ookayama, Meguro, Tokyo 152, Japan

Z. Naturforsch. **34a**, 600–608 (1979); received March 3, 1979

A Green's function perturbation technique is presented which is appropriate for studying the chemisorption behavior of ordered atomic layers on a metal surface. The phase shift technique is used to determine the change in the electronic density of states due to chemisorption. The method is quite general and can be used to study the electronic structure of arbitrary ordered overlayers. Numerical results are given for $p(2\times2)$, $c(4\times2)$, $p(2\times1)$, $c(2\times2)$ and $p(1\times1)$ overlayers on a (001) surface of a tight-binding fcc metal. It is shown that the effects of long-range order and the binding geometry of the adsorbate layer are of great importance for the electronic structure of ordered overlayers.

1. Introduction

In order to develop a qualitative picture of the complex chemisorption process, simple model calculations have been very useful. Using Green's functions coupled with the phase shift technique, several authors have studied the single atom chemisorption on the various surfaces [1–3]. Recently, the model calculations were extended to consider a monolayer of adatoms. Ho, Cunningham and Weinberg [4, 5] have investigated the change in the electronic density of states (DOS) due to the adsorption of a monolayer of atoms ($\theta=1$) on the (001) surface both of a model bcc metal (one-band) and of a model two-band crystal with the CsCl structure. The present author has studied the effect of having the monolayer of atoms on the tight-binding metal surface, using the two-peaked DOS model for the substrate [6]. Ideally, however, the calculation should be carried out considering ordered overlayers with general coverage since the surface superstructures are found in many chemisorption systems by low energy electron diffraction [7]; e.g., $c(2\times2)$-H structure on W(001) and Mo(001) surface, (2×1)-O structure on Ir(001), Ni(110) and Pt(110) and $c(4\times2)$-CO structure on Pd(001) and Pt(001) surfaces.

In the present paper, we investigate the chemisorption behavior for the ordered overlayers with $\theta=1/4$ and $1/2$ (most frequently observed overlayer structures) on the (001) surface of a fcc tight-binding metal. For comparison, we also investigate the chemisorption behavior for the single adatom ($\theta\approx0$) and the monolayer ($p(1\times1)$ overlayer) of adatoms. The fcc metal is chosen from the following considerations: (1) There has been a considerable amount of experimental work dealing with the adsorption of ordered atomic layers on the fcc metal surfaces (see Table 1). (2) A simple modification of the present theory can be used to study the adsorption behavior on the reconstructed surface [8, 9] or on the surface with relaxation [10]; the occurence of surface reconstruction (or surface relaxation) is a commonly observed phenomenon in fcc metals. The present calculation, then, will be important as a basis for comparison with these other related calculations.

The present method uses the Linear Combination of Atomic Orbitals (LCAO) scheme and the tight-binding approximation to describe the electronic structure of a semi-infinite crystal. The tight-bind-

Table 1. Ordered overlayers with $\theta=1/4$ and $1/2$ on the fcc transition metal surfaces (from Somorjai, Ref. [7], $*\theta=1.0$).

substrate	superstructure	substrate	superstructure
Ir(100)	(2×1)–O	Ni(110)	(2×1)–O
	$c(2\times2)$–CO		(1×2)–H
Ni(100)	(2×2)–O		(1×1)–CO*
	$c(2\times2)$–O	Pd(110)	(1×2)–O
	(2×2)–CO		$c(2\times4)$–O
	$c(2\times2)$–CO		(2×1)–CO
Pd(100)	$c(4\times2)$–CO	Pt(110)	(2×1)–O
Pt(100)	$c(4\times2)$–CO	Rh(110)	$c(2\times4)$–O
	(2×2)–H		(2×2)–O
	(1×1)–CO*		$c(2\times2)$–O
			(1×2)–O

Reprint requests to Prof. Kin-ichi Masuda. Please order a reprint rather than making your own copy.

0340-4811 / 79 / 0500-0600 $ 01.00/0

ing model is known to give a better idea of the d-band properties of transition metals than the electron gas model. The electronic DOS for the clean substrate layers is obtained by the method developed by Allan [11] and Kalkstein and Soven [12] (AKS). Each adatom is represented by a single non-degenerate energy level E_a. Two binding sites, the on-site and the centered fourfold-site, are considered. The Green's function perturbation technique and the phase shift function approach are used to calculate the change in the electronic DOS, $\Delta\varrho(E)$, during chemisorption. The calculation of $\Delta\varrho(E)$ is quite important since it is directly applicable to photo-emission. It is noted that no other method gives the same information in such a straightforward manner.

In Sect. 2, we present the formulation for obtaining the chemisorbed Green's function and the change in the DOS, $\Delta\varrho(E)$, due to chemisorption for the ordered overlayers with $\theta = 1/4$ and $1/2$. However, the extension to other ordered overlayers is straightforward. Section 3 contains the results and discussion of numerical calculations. In this section, we demonstrate that the effects of the long-range order and the binding geometry of the adsorbate layer are of great importance for the electronic structure of ordered overlayers. The final Sect. 4 is devoted to conclusions.

2. Model and Formulation

In the following we consider the adatom/substrate binding from the standpoint of the Newns-Anderson model [13, 14]. We assume that chemisorbed atoms form a simple superstructure coherent to the unreconstructed substrate surface layer. One can therefore construct the two-dimensional (2D) Brillouin Zone (ABZ) corresponding to the ordered adsorbate lattice in the surface Brillouin Zone (SBZ).

2.1. Ordered Overlayers with $\theta = 1/2$

We consider the $p(2\times 1)$ and $c(2\times 2)$ overlayers on the (001) surface of a fcc tight-binding metal. The bulk band structure of this metal is given by

$$\begin{aligned} E(k) = &-4\,|\gamma|\cdot[\cos(k_x/2)\cos(k_y/2) \\ &+\cos(k_y/2)\cos(k_z/2) \\ &+\cos(k_z/2)\cos(k_x/2)]\,, \end{aligned} \tag{1}$$

where γ is the hopping integral between the nearest-neighbour atoms and lattice constant a is set equal to unity. In Fig. 1, we show the geometry and the ABZ for the $p(2\times 1)$ and $c(2\times 2)$ overlayers. For both overlayers, the first ABZ has one-half the area of the first SBZ (unreconstructed clean surface). We denote the wave vectors inside the first ABZ as $k_\parallel$ and those inside the first SBZ as $k_\parallel{}^s$. Then, for a given $k_\parallel$ in ABZ, there are $q\,k_\parallel{}^s$'s in SBZ that are expressed as $k_\parallel{}^s = k_\parallel + K_h$, where K_h is a reciprocal lattice wave vector of the ordered adsorbate lattice and $q = 2(4)$ for the overlayers with $\theta = 1/2(1/4)$ [15].

For convenience, we construct the layered Bloch orbitals as

$$|0, k_\parallel\rangle = N_a^{-1/2}\sum_{R_a}\exp(i\,k_\parallel\cdot R_a)\,|R_a\rangle\,, \tag{2}$$

$$\begin{aligned} &|n, k_\parallel{}^s\rangle \\ &= (q N_a)^{-1/2}\sum_{R_{sn}}\exp[i(k_\parallel + K_h)\cdot R_{sn}]\,|R_{sn}\rangle\,, \end{aligned} \tag{3}$$

where N_a is the number of adatoms, $R_{sn}(R_a)$ is the position vectors of the substrate (adsorbate) atoms in the n-th substrate layer and $|R_{sn}\rangle$ ($|R_a\rangle$) denotes localized wave functions centered on lattice site $R_{sn}(R_a)$. In terms of these layered Bloch orbitals, the perturbation (adsorbate-substrate hopping interaction) matrix elements, $V_{as}(k_\parallel + K_h)$ and $V_{sa}(k_\parallel + K_h)$ $[= V_{as}^{\dagger}(k_\parallel + K_h)]$, can be written as

$$V_{as}(k_\parallel + K_h) = V_t/\sqrt{q}\,, \tag{4a}$$

for the on-site adsorption

$$\begin{aligned} &= 2\,V_c/\sqrt{q}\,[\cos(k_x + K_{hx})/2 \\ &\quad + \cos(k_y + K_{hy})/2]\,, \end{aligned} \tag{4b}$$

for the centered fourfold-site adsorption, where $V_t(V_c)$ denotes the on-site (centered fourfold-site) adatom-substrate atom binding strength.

In order to derive the partial ($k_\parallel$ dependent) phase shift function [16, 17], one further requires the knowledge of the unperturbed Green's function matrix $\tilde{G}^0(k_\parallel, E)$. When the direct interaction between the adatoms can be neglected, the unperturbed Green's function for the adatom, $G_{aa}^0(k_\parallel, E)$ is written as

$$G_{aa}^0(k_\parallel, E) \equiv G_{aa}^0(E) = [E - E_a + i\,0]^{-1}. \tag{5}$$

On the other hand, the unperturbed (clean) surface Green's function appropriate for the $p(2\times 1)$ and $c(2\times 2)$ overlayers is obtained from the AKS formalism and is given for the (001) surface of a

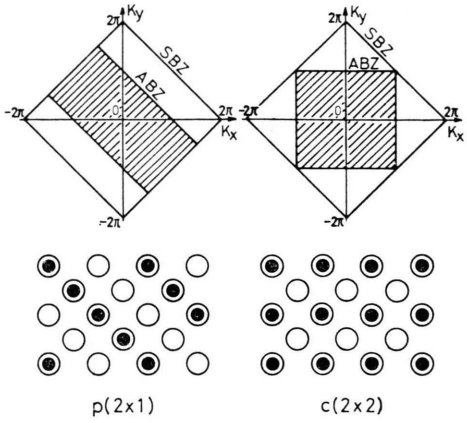

Fig. 1. Two-dimensional Brillouin Zones appropriate for the (001) surface of the fcc lattice (SBZ) and the ordered adsorbate lattice (ABZ) with $\theta = 1/2$, $p(2\times 1)$ and $c(2\times 2)$ structures. The lattice constant a is set equal to unity.

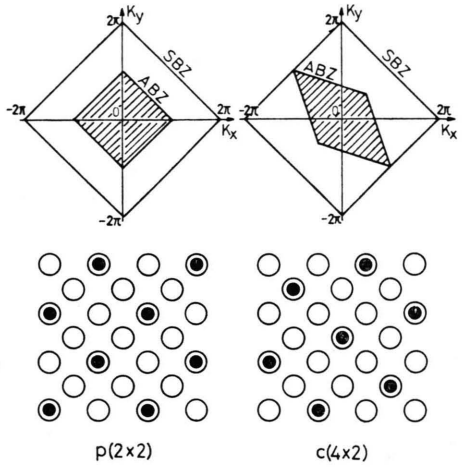

Fig. 2. The fcc(001) surface Brillouin Zone and ABZ for $p(2\times 2)$ and $c(4\times 2)$ overlayers.

fcc tight-binding metal as

$$G^0_{ss}(k_\parallel + K_h, E) = [W(k_\parallel + K_h) - i\{4|T(k_\parallel + K_h)|^2 - W^2(k_\parallel + K_h)\}^{1/2}]/2|T(k_\parallel + K_h)|^2, \quad (6)$$

where $\{4|T|^2 - W^2\}^{1/2}$ must be interpreted as $-i\cdot\mathrm{sgn}(W)\{W^2 - 4|T|^2\}^{1/2}$ for $W^2 > 4|T|^2$ and

$$W(k_\parallel + K_h) = E - 4\gamma\cos\{(k_x + K_{hx})/2\}\cdot\cos\{(k_y + K_{hy})/2\}, \quad (7)$$

$$T(k_\parallel + K_h) = -2\gamma[\cos\{(k_x + K_{hx})/2\} + \cos\{(k_y + K_{hy})/2\}]. \quad (8)$$

Following the phase shift technique [16, 17], we determine the partial ($k_\parallel$ dependent) phase shift function for the ordered overlayers. This phase shift function $\eta_\chi(k_\parallel; E)$ is given by

$$\eta_\chi(k_\parallel, E) = -\arg\cdot\det[\tilde{I} - \tilde{V}_\chi \tilde{G}_\chi{}^0(k_\parallel, E)], \quad (9)$$

where the subscript χ becomes t or c for the on-site or centered fourfold-site geometry, respectively, $\tilde{I}$ is the unit matrix, and $\tilde{V}$ and $\tilde{G}^0$ are the perturbation and the unperturbed Green's function matrices, respectively. After a short calculation, one finds that the partial phase shift functions for the $p(2\times 1)$ overlayer are given by

$$\eta_t(k_\parallel, E) = -\arg[1 - (V_t{}^2/2)\{G^0_{ss}(k_x, k_y, E) + G^0_{ss}(\pi - k_x, \pi - k_y, E)\}G^0_{aa}(E)], \quad (10)$$

$$\eta_c(k_\parallel, E) = -\arg[1 - (V_c{}^2/2)\{4(\cos(k_x/2) + \cos(k_y/2))^2 G^0_{ss}(k_x, k_y, E) + 4(\sin(k_x/2) + \sin(k_y/2))^2 \cdot G^0_{ss}(\pi - k_x, \pi - k_y; E)\}G^0_{aa}(E)]. \quad (11)$$

The corresponding η_χ expressions for the $c(2\times 2)$ overlayers are written as

$$\eta_t(k_\parallel, E) = -\arg[1 - (V_t{}^2/2)\{G^0_{ss}(k_x, k_y, E) + G^0_{ss}(2\pi - k_x, k_y, E)\}G^0_{aa}(E)], \quad (12)$$

$$\eta_c(k_\parallel, E) = -\arg[1 - (V_c{}^2/2)\{4(\cos(k_x/2) + \cos(k_y/2))^2 G^0_{ss}(k_x, k_y, E) + 4(\cos(k_y/2) - \cos(k_x/2))^2 \cdot G^0_{ss}(2\pi - k_x, k_y, E)\}G^0_{aa}(E)]. \quad (13)$$

Once the partial phase shift function is known, the change in the electronic DOS, $\Delta\varrho(E)$, can be given by

$$\Delta\varrho(E) = (1/\pi)\cdot\partial\eta_\chi(E)/\partial E, \quad (14)$$

where the total phase shift function $\eta_\chi(E)$ is defined by

$$\eta_\chi(E) = \{(1/N_a)\sum_{k_x, k_y}\eta_\chi(k_x, k_y, E)\} - \pi\,\theta(E_a - E). \quad (15)$$

Here, the summation over k_x and k_y extends over the first ABZ and the Heaviside theta function is added so that $\Delta\varrho(E)$ directly gives the difference in the DOS between the chemisorbed system and the clean substrate. In Eq. (14), we find the sum rule

$$\int_{-\infty}^{+\infty}\Delta\varrho(E)\,dE = 1, \quad (16)$$

since we are adding an electron state to the system. In addition, it is important to realize that $\Delta\varrho(E)$ in Eq. (14) is the quantity of experimental interest since photoemission difference spectra are obtained by subtraction of the clean substrate spectrum from the chemisorbed system spectrum.

The chemisorbed Green's function is obtained by solving the matrix-form Dyson equation:

$$\tilde{G} = \tilde{G}^0 + \tilde{G}^0 \tilde{V} \tilde{G} . \tag{17}$$

The explicit expression of the chemisorbed Green's function is written, in a mixed Bloch-Wannier representation, as follows: For the $p(2\times 1)$ overlayer ($K_h = (0,0)$ and $(-\pi, -\pi)/a$), the adsorbate Green's function is given by

$$G_t(k_\parallel, E; 0, 0) = [E - E_a - (V_t^2/2)\{G_{ss}^0(k_x, k_y, E) + G_{ss}^0(\pi - k_x, \pi - k_y, E)\}]^{-1} , \tag{18}$$

$$G_c(k_\parallel, E; 0, 0) = [E - E_a - (V_c^2/2)\{4(\cos(k_x/2) + \cos(k_y/2))^2 G_{ss}^0(k_x, k_y, E) + 4(\sin(k_x/2) + \sin(k_y/2))^2 \cdot G_{ss}^0(\pi - k_x, \pi - k_y, E)\}]^{-1} . \tag{19}$$

The similar expressions of the adsorbate Green's function are obtained for the $c(2\times 2)$ overlayer ($K_h = (0,0)$ and $(-2\pi, 0)/a$). On the other hand, the chemisorbed Green's function for the substrate layer ($n = 1, 2, 3, \ldots$) is written as

$$G_\chi(k_\parallel + K_h, E; 1, 1) = \frac{1}{W - |T|^2 G_{ss}^0(k_\parallel + K_h, E) - |V_{as}(k_\parallel + K_h)|^2 / D(k_\parallel, E)} , \tag{20}$$

$$G_\chi(k_\parallel + K_h, E; 2, 2) = \frac{1}{W - |T|^2 G_{ss}^0(k_\parallel + K_h, E) - |T|^2 / [W - |V_{as}(k_\parallel + K_h)|^2 / D(k_\parallel, E)]} , \tag{21}$$

$$G_\chi(k_\parallel + K_h, E; 3, 3) = \cdots , \tag{22}$$

where

$$D(k_\parallel, E) = E - E_a - \sum_{K_q \neq K_h} |V(k_\parallel + K_q)|^2 \cdot G_{ss}^0(k_\parallel + K_q, E) , \tag{23}$$

and $W \equiv W(k_\parallel + K_h)$ and $T \equiv T(k_\parallel + K_h)$ are defined by Eqs. (7) and (8), respectively. The local electronic DOS of the chemisorbed system can be calculated by the usual formula

$$\varrho_a(E) = -(1/\pi N_a) \sum_{k_x, k_y} \operatorname{Im} G_\chi(k_\parallel, E; 0, 0) , \tag{24}$$

$$\varrho_n(E) = -(1/\pi q N_a) \sum_{k_x, k_y} \sum_{K_h} \operatorname{Im} G_\chi(k_\parallel + K_h, E; n, n) . \tag{25}$$

2.2. *Ordered Overlayers with $\theta = 1/4$*

Two different ordered structures of the adsorbate layer are considered here. The adatoms are arranged in two different ways forming the $p(2\times 2)$ and the $c(4\times 2)$ structures. In Fig. 2, we show the geometry and the ABZ for the $p(2\times 2)$ and $c(4\times 2)$ overlayers. For the ordered overlayers, four different reciprocal lattice vectors K_h are required to satisfy the relation $k_\parallel^s = k_\parallel + K_h$, since the real space unit cell of the overlayers with $\theta = 1/4$ is four times larger than that of the clean substrate layer.

For the $p(2\times 2)$ overlayer, K_h are given in units of a^{-1} as

$$K_h = (0,0),\ (-\pi, -\pi),\ (\pi, -\pi) \quad \text{and} \quad (0, -2\pi) . \tag{26}$$

Thus, one can obtain the partial phase shift function for the $p(2\times 2)$ overlayer

$$\eta_t(k_\parallel, E) = -\arg[1 - (V_t^2/4)\{G_{ss}^0(k_x, k_y, E) + G_{ss}^0(\pi - k_x, \pi - k_y, E) + G_{ss}^0(\pi + k_x, \pi - k_y, E) + G_{ss}^0(k_x, 2\pi - k_y, E)\} G_{aa}^0(E)] , \tag{27}$$

$$\eta_c(k_\parallel, E) = -\arg[1 - (V_c^2/4)\{4(\cos(k_x/2) + \cos(k_y/2))^2 G_{ss}^0(k_x, k_y, E) + 4(\sin(k_x/2) + \sin(k_y/2))^2 \cdot G_{ss}^0(\pi - k_x, \pi - k_y, E) + 4(\sin(k_y/2) - \sin(k_x/2))^2 \cdot G_{ss}^0(\pi + k_x, \pi - k_y, E) + 4(\cos(k_x/2) - \cos(k_y/2))^2 \cdot G_{ss}^0(k_x, 2\pi - k_y, E)\} G_{aa}^0(E)] . \tag{28}$$

On the other hand, for the $c(4\times 2)$ overlayer the reciprocal lattice wave vectors K_h are given as

$$K_h = (0,0),\ (-3\pi/2, \pi/2),\ (-3\pi, \pi) \quad \text{and} \quad (-9\pi/2, 3\pi/2) . \tag{29}$$

Using these reciprocal lattice vectors K_h, one obtains the following expressions for the phase shift function

$$\eta_t(k_\parallel, E) = -\arg[1 - (V_t^2/4)\{G_{ss}^0(k_x, k_y, E) + G_{ss}^0(3\pi/2 - k_x, \pi/2 + k_y, E) + G_{ss}^0(3\pi - k_x, \pi + k_y, E) + G_{ss}^0(9\pi/2 - k_x, 3\pi/2 + k_y, E)\} G_{aa}^0(E)] , \tag{30}$$

$$\eta_c(k_\parallel, E) = -\arg[1 - (V_c^2/4)\{4(\cos(k_x/2) + \cos(k_y/2))^2 G_{ss}^0(k_x, k_y, E) + 2[\sin(k_x/2) - \sin(k_y/2) - (\cos(k_x/2) - \cos(k_y/2))]^2 \cdot G_{ss}^0(3\pi/2 - k_x, \pi/2 + k_y, E) + 4(\sin(k_x/2) + \sin(k_y/2))^2 \cdot G_{ss}^0(3\pi - k_x, \pi + k_y, E) + 2(\sin(k_x/2) - \sin(k_y/2) + \cos(k_x/2) - \cos(k_y/2))^2 \cdot G_{ss}^0(9\pi/2 - k_x, 3\pi/2 + k_y, E)\} G_{aa}^0(E)]\,. \quad (31)$$

The calculations of the change in the electronic DOS, $\Delta\varrho(E)$, due to chemisorption and the adsorbate (substrate) electronic structure are similar to those for the p(2×1) and c(2×2) overlayers.

3. Calculation Results and Discussions

In this section we present the adsorbate electronic structure, $\varrho_a(E)$, and the change in the DOS, $\Delta\varrho(E)$, due to chemisorption for the p(2×2), c(4×2), p(2×1) and c(2×2) overlayers on the (001) surface of the tight-binding fcc metal using the method described in the previous section. These ordered overlayers are observed in the adsorption of simple atoms on the low index surface planes of fcc transition metals (Table 1). For comparison, we also present the corresponding results for the single adatom and the monolayer of adatoms (p(1×1) overlayer). The computation is performed for the two adsorption sites, the on-site and centered fourfold-site.

The electronic structure of the clean surface (clean surface Green' function) of the tight-binding fcc metal is calculated by the use of the AKS formalism [11, 12]. In Figs. 3a and 3b, we present the real and imaginary parts of the surface Green's function appropriate for the on-site and centered fourfold-site adsorption. The energy is given in units of $2|\gamma|$ (the bandwidth is 8). The surface Green's function for the centered fourfold-site adsorption is calculated from

$$G_{ss}^c(E) = \frac{1}{(4\pi)^2}\int_{-2\pi}^{2\pi} dk_x^s \int_{-2\pi}^{2\pi} dk_y^s\, G_{ss}^0(k_x^s, k_y^s, E) \cdot \{1 + 2\cos(k_x^s/2)\cos(k_y^s/2) + \cos(k_x^s)\}\,, \quad (32)$$

where $G_{ss}^0(k_x^s, k_y^s, E)$ is defined by Equation (6). One can see that the general feature of Im $G_{ss}^c(E)$ is considerably different from that for the on-site adsorption; Im $G_{ss}^c(E)$ curve indicates the downward shift in energy of the symmetrized surface Wannier states. These Green's function curves are helpful when discussing the chemisorption behaviors.

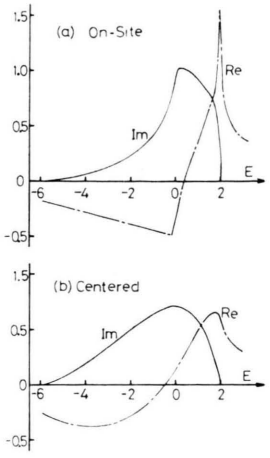

Fig. 3. Real (dot-dashed) and imaginary (solid) parts of Green's function appropriate for single atom adsorption on the (001) surface of an fcc metal; on-site (a) and centered fourfold-site (b) adsorption. The energies are given in units of $2|\gamma|$.

Before discussing the general behavior of $\varrho_a(E)$ and $\Delta\varrho(E)$, we investigate the behaviors of the localized electronic states for the ordered overlayers. In general, the existence of localized states alters the chemisorption behavior drastically. It is well known that the adsorption of atoms to a surface can introduce electronic states which are localized outside the energy band. The localized electronic states exist if there are solutions of the following Equation [18]:

$$\det \| \tilde{I} - \tilde{V}_\chi \cdot \tilde{G}_\chi{}^0(k_x, k_y, E) \| = 0\,, \quad (33)$$

for values of E which lie outside the energy bands when plotted in $k_\parallel$ space. Thus, one can see that the localized states for the ordered overlayers are wave vector $k_\parallel$ dependent. In the case of the single atom adsorption, the localized states exsist as a delta function outside the extrema of the band, i.e., the split-off states from the band edges.

In Fig. 4, we show the positions of the localized electronic states for the p(2×1) overlayer with respect to the energy band along the particular segment in the SBZ, $k_y = k_x + 3\pi/2$, $-3\pi/4 \leqq k_x \leqq \pi/4$. For the on-site adsorption (Fig. 4a) with $E_a = 0$ and $V_t = 1.5$ (similar values of V_t have been used in Refs. [1–6]), the localized states exist both

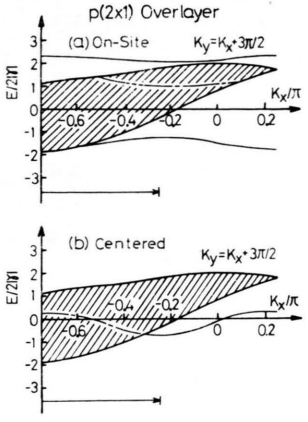

Fig. 4. The positions of the localized electronic states for the $p(2\times1)$ overlayer on the fcc(001) surface along the segment, $k_y = k_x + 3\pi/2$, $-3\pi/4 \leqq k_x \leqq \pi/4$. Also shown (dot-dashed) are the positions of the "virtual states". The arrows below the figures (a) and (b) indicate the boundary of the ABZ.

above and below the band. These states are derived from the anti-bonding split-off states and bonding split-off states, respectively. In Fig. 4, we also show the position of the "virtual (localized) states" (dot-dushed curve) which are given by the solutions of the equation

$$\text{Re det} \parallel \tilde{I} - \tilde{V}_\chi \cdot \tilde{G}_\chi{}^0(k_x, k_y, E) \parallel = 0\,, \qquad (34)$$

inside the energy bands. The existence of the "virtual states" can also alter the chemisorption behavior considerably as will be shown later. As can be seen in Fig. 4a, there are "virtual states" for the $p(2\times1)$ overlayer with the on-site adsorption. For the centered fourfold-site adsorption (Fig. 4b), with $E_a = 0$ and $V_c = 0.75$ $(= V_t/2)$, the localized states exist only below the band. Here, it is noted that in order to consider the same total binding strength for the two adsorption sites (on-site and centered fourfold-site), one must choose $V_c = V_t/2$ [2, 4, 5]. Furthermore, for the centered fourfold-site adsorption there are no "virtual states". These dramatic differences in the localized (or "virtual") states behavior between the on-site and centered fourfold-site adsorptions are important when interpreting the calculation results of $\Delta\varrho(E)$. The general behavior of the localized and "virtual" states for the $p(2\times2)$, $c(4\times2)$ and $p(1\times1)$ overlayers is similar to that for the $p(2\times1)$ overlayer. For the $c(2\times2)$ overlayer, however, the appearance of the localized and "virtual" states is different from that of the other, i.e., for this overlayer, there are no "virtual states" both for the on-site and centered fourfold-site adsorptions.

In Fig. 5, we present the adsorbate electronic structure, $\varrho_a(E)$, and the change in the electronic DOS, $\Delta\varrho(E)$, due to the on-site adsorption of the ordered atomic layers with $\theta = 1/4$ and $1/2$, together with the results for the single adatom and the monolayer of adatoms; all energies are expressed in units of $2|\gamma|$ and the parameter values, $E_a = 0$ and $V_t = 1.5$, are used. These $\varrho_a(E)$ and $\Delta\varrho(E)$ curves show the familiar bonding and anti-bonding resonances in the surface density of states and how these resonances are affected by changes in the coverage and structure of the overlayers. In general, as the adsorbate coverage increases, the $\Delta\varrho(E)$ curve differs more significantly from the corresponding curve for the single atom adsorption: Note that the bonding and anti-bonding resonance peaks for the ordered overlayers are strongly skewed compared to those for the single atom adsorption. This

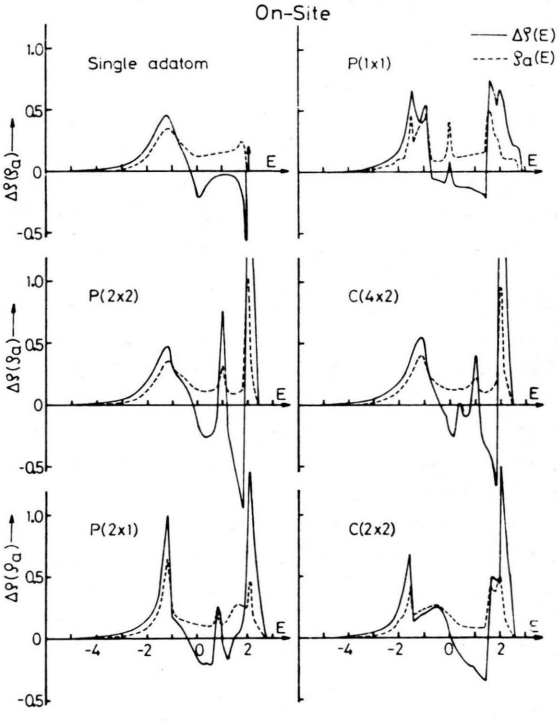

Fig. 5. The change in the electronic DOS, $\Delta\varrho(E)$, per adatom and the adsorbate electronic structure, $\varrho_a(E)$, for a single adatom and $p(2\times2)$, $c(4\times2)$, $p(2\times1)$, $c(2\times2)$ and $p(1\times1)$ overlayers on an fcc(001) surface. The adatoms ($E_a = 0$) are situated in the on-site positions. $V_t = 1.5$. The arrow in the $\Delta\varrho(E)$ (or $\varrho_a(E)$) curve for the single adatom indicates the localized antibonding (split-off) state.

results from the fact that the localized electronic states for the ordered overlayers are wave vektor $k_{\|}$ dependent. Thus, the indirect interactions between the adatoms are very important for the electronic structure of the overlayers.

Furthermore, for the $p(2\times2)$, $c(4\times2)$, $p(2\times1)$ and $p(1\times1)$ overlayers, one can observe the prominent non-bonding resonance peaks near the adsorbate energy level E_a. The appearance of the non-bonding resonance peak near E_a for these overlayers is due to the existence of the "virtual states" (Eq. (34)) and is significant in the $\Delta\varrho(E)$ curves. Therefore, the existence of the "virtual states" is as important as that of the true localized states in the calculation of $\Delta\varrho(E)$.

The adsorbate electronic structure, $\varrho_a(E)$, and the change in the electronic DOS, $\Delta\varrho(E)$, for the centered fourfold-site adsorption are shown in Fig. 6 with $E_a=0$ and $V_c=0.75$ $(=V_t/2)$. In contrast to the on-site adsorption, the centered fourfold-site $\Delta\varrho(E)$ $[\varrho_a(E)]$ curves show the two

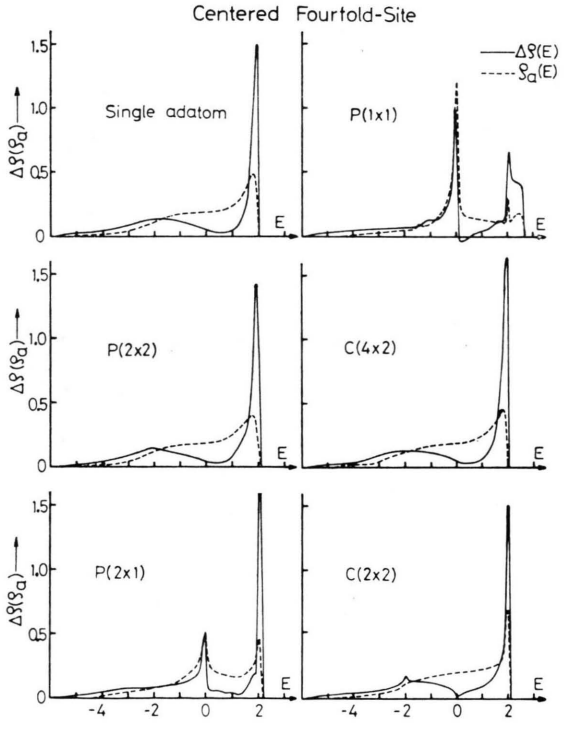

Fig. 6. The change in the electronic DOS, $\Delta\varrho(E)$, and the adsorbate electronic structure, $\varrho_a(E)$, for a single adatom and $p(2\times2)$, $c(4\times2)$, $p(2\times1)$, $c(2\times2)$ and $p(1\times1)$ overlayers on an fcc(001) surface. The adatoms ($E_a=0$) are situated in the centered fourfold-site positions. $V_c=0.75$ $(=V_t/2)$.

peaked structure with the bonding and anti-bonding resonances, irrespective of the type of the overlayers. For the $p(2\times2)$, $c(4\times2)$ and $c(2\times2)$ overlayers, the bonding and anti-bonding resonance peaks are located considerably below and above the adsorbate energy level E_a. However, for the $p(2\times1)$ and $p(1\times1)$ overlayers, the bonding resonance peaks are located at the adsorbate energy level. Since the usual bonding resonance peaks are observed below the adsorbate energy (in the present case $E_a=0$), these bonding states at E_a are different in nature from the usual bonding states, i.e., the bonding states for the $p(2\times2)$, $c(4\times2)$ and $c(2\times2)$ overlayers. Since the resonance peak at the adsorbate energy level is ineffective for the formation of the strong chemisorption bond, these bonding states for the $p(2\times1)$ and $p(1\times1)$ overlayers are referred to as the non-bonding states in the following. The appearance of the non-bonding states at the adsorbate energy level is explained as follows: For the $p(2\times1)$ overlayer with centered fourfold-site adsorption, the values both of $V_{as}(k_{\|})$ and $V_{as}(k_{\|}+K_h)$ vanish at the zone boundary of ABZ, $k_y=k_x\pm2\pi$, $\mp\pi/4\leqq k_x\leqq\mp3\pi/4$. On the other hand, for the $p(1\times1)$ overlayer, the values of $V_{as}(k_{\|}{}^s)$ vanish at the zone boundary of SBZ. Therefore, the electronic states with these $k_{\|}$ (or $k_{\|}{}^s$) have no interaction between the overlayer and the substrate layer and thus have the degenerate energy $E=E_a$. From this, one can see that these non-bonding states do not occur for the on-site adsorption.

Summarizing these features of the $\Delta\varrho(E)$ $[\varrho_a(E)]$ curves, the following should be pointed out: (1) By examining the coverage dependence of the resonance peaks, it is possible to get information about the chemisorption binding site and the structure of the overlayers. (2) The non-bonding states (at and near E_a) for the ordered overlayers are essentially different in nature from those for the single atom chemisorption of Refs. [19, 20], where the non-bonding peak appears due to the minimum in the substrate DOS.

Finally, we briefly discuss the electronic structure for the atoms in the substrate layers. The local DOS for the atoms in the first three atomic layers are calculated from Equations (20)—(25). In Fig. 7, we show the substrate electronic structure, $\varrho_n(E)$, $n=1, 2,$ and 3, for the $c(2\times2)$ overlayer with on-site adsorption. One can clearly observe the

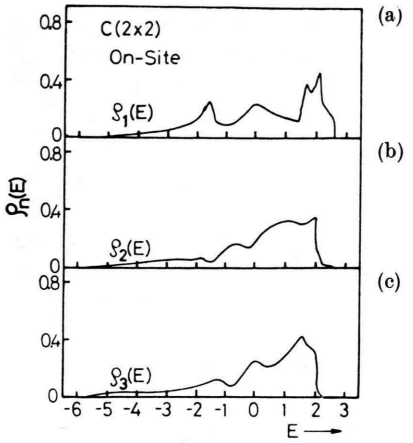

Fig. 7. Local DOS per atom for the first three substrate layers in the presence of the (001) surface covered with adatoms in on-site positions in the $c(2\times 2)$ superstructure. $E_a = 0$, $V_t = 1.5$. $n = 1$ (a), 2 (b) and 3 (c).

bonding and anti-bonding resonance peaks only for the first substrate layer and not clearly observe for the second and third substrate layers. This indicates that the chemisorption bonds are well localized between the adsorbate and first substrate layers. This feature of the substrate electronic structure is common to the other overlayers.

4. Conclusions

We have investigated the chemisorption behavior for ordered overlayers with $\theta = 1/4$ and $1/2$ on the (001) surface of the model fcc transition (single s-band tight-binding model) metal. For comparison, we have also investigated the chemisorption behavior for a single adatom and a monolayer of adatoms. The calculations of the adsorbate electronic structure, $\varrho_a(E)$, and the change in the electronic DOS, $\Delta\varrho(E)$, due to chemisorption have been performed for a single adatom and $p(2\times 2)$, $c(4\times 2)$, $p(2\times 1)$, $c(2\times 2)$ and $p(1\times 1)$ overlayers, considering the two different binding sites, the on-site and the centered fourfold-site.

In general, we have found that the results for $\varrho_a(E)$ and $\Delta\varrho(E)$ depend strongly on the adsorbate coverage, structure of the ordered overlayers, and the adsorption geometry (on-site and centered fourfold-site bindings). Both for the on-site and centered fourfold-site adsorption, the $\Delta\varrho(E)$ and $\varrho_a(E)$ curves differ more significantly from the corresponding curves for the single atom adsorption as the adsorbate coverage θ increases: The resonance peaks for the ordered overlayers are strongly skewed compared to those for the single atom adsorption. This implies that indirect interactions between the adatoms play the leading role in the chemisorption of ordered atomic layers. Furthermore, the results of $\Delta\varrho(E)$ [$\varrho_a(E)$] for the $c(2\times 2)$ ($c(4\times 2)$) overlayer are significantly different from those for the $p(2\times 1)$ ($p(2\times 2)$) overlayer. This indicates that the long range order of the adsorbate layer is of great importance for the electronic structure of the ordered overlayers. It has been in fact observed that $\Delta\varrho(E)$ is sensitive to the adlayer structure: photoemission and INS spectra for systems such as O/Ni(001) and Te/Ni(001) [21].

The present work has also shown that two kinds of non-bonding peaks (at and near E_a) appear in the $\Delta\varrho(E)$ curves for ordered overlayers with $\theta = 1/4$ and $1/2$. The non-bonding resonance peaks at the adsorbate energy level E_a appear due to the symmetry of the adlayer (centered fourfold-site adsorption) while those near E_a result from the existence of "resonance electronic states".

Finally, we note that the present results will serve as the basis for comparison to similar chemisorption calculations which will be carried out for a reconstructed surface or a surface with relaxation. These calculations are of considerable importance for the understanding of the mechanism of the impurity (adatom)-stabilized unreconstructed surface or the mechanism of the adatom-induced surface relaxation [9, 10].

Acknowledgement

The author is very grateful to the Sakkokai Foundation for the financial support.

[1] T. L. Einstein, Surf. Sci. **45**, 713 (1974); Phys. Rev. **B 12**, 1262 (1975).
[2] W. Ho, S. L. Cunningham, and W. H. Weinberg, J. Vac. Sci. Technol. **13**, 349 (1976); Surf. Sci. **54**, 139 (1976).
[3] K. Masuda, Z. Naturforsch. **31a**, 1344 (1976); Comm. Phys. **2**, 77 (1977).
[4] W. Ho, S. L. Cunningham, and W. H. Weinberg, Surf. Sci. **62**, 662 (1977).
[5] W. Ho, S. L. Cunningham, and W. H. Weinberg, Surf. Sci. **66**, 495 (1977).

[6] K. Masuda, phys. stat. sol. **87b**, 739 (1978).
[7] G. A. Somorjai, Surf. Sci. **34**, 156 (1973).
[8] G. A. Somorjai and H. H. Farrell, Adv. Chem. Phys. **20**, 215 (1971); A. Ignatiev, A. V. Jones, and T. N. Rhodin, Surf. Sci. **30**, 573 (1972).
[9] C.-M. Chan, S. L. Cunningham, K. L. Luke, W. H. Weinberg, and S. P. Withrow, Surf. Sci. **78**, 15 (1978); C.-M. Chan, K. L. Luke, M. A. Van Hove, W. H. Weinberg, and S. P. Withrow, Surf. Sci. **78**, 386 (1978).
[10] J. F. Van Der Veen, R. G. Smeenk, R. M. Tromp, and F. W. Saris, Surf. Sci. **79**, 212 (1979).
[11] G. Allan, Ann. Phys. Paris **5**, 169 (1970).
[12] D. Kalkstein and P. Soven, Surf. Sci. **26**, 85 (1971).
[13] T. B. Grimley, Proc. Roy. Soc. London **90**, 757 (1967); **92**, 776 (1967).
[14] D. M. Newns, Phys. Rev. **178**, 1123 (1969).
[15] Y. Muda and T. Hanawa, Surf. Sci. **66**, 145 (1977).
[16] G. Toulouse, Solid State Commun. **4**, 593 (1966).
[17] L. Dobrzynski and D. L. Mills, Phys. Rev. **B 7**, 2367 (1973); R. E. Allen, Surf. Sci. **76**, 91 (1978).
[18] J. Callaway, J. Math. Phys. **5**, 783 (1964); G. Allan and P. Lenglart, Surf. Sci. **30**, 641 (1972).
[19] S. K. Lyo and R. Gomer, Phys. Rev. **B 10**, 4161 (1974); T. B. Grimley, Prog. Surf. Membrane Sci. **9**, 71 (1975).
[20] K. Masuda, Z. Naturforsch. **33a**, 66 (1978).
[21] H. D. Hagstrum and G. E. Baker, Orbital Energy Spectra Produced by Adsorbed Atoms, in Battelle Colloquium, Gstaad 1974; D. E. Eastman and J. K. Cashion, Phys. Rev. Lett. **27**, 1520 (1971); R. H. Paulson and T. N. Rhodin, Surf. Sci. **55**, 61 (1976).